Spatiotemporal three-dimensional mapping of nonlinear X waves

J. Trull,* O. Jedrkiewicz, and P. Di Trapani

INFM and Department of Chemical, Physical and Mathematical Sciences, University of Insubria, Via Valleggio 11, 22100 Como, Italy

A. Matijosius, A. Varanavicius, G. Valiulis, R. Danielius, E. Kucinskas, and A. Piskarskas

Department of Quantum Electronics, Vilnius University Sauletekio 9, bldg. III, LT-2040 Vilnius, Lithuania

S. Trillo

*Department of Engineering, University of Ferrara, Via Saragat 1, 44100 Ferrara, Italy
and Istituto Nazionale di Fisica della Materia–RM3, Via della Vasca Navale 84, 00146 Roma, Italy*

The spatiotemporal intensity profile of a 100-fs wave packet at the output of a $X^{(2)}$ crystal, tuned for mismatched second-harmonic generation, is probed via sum-frequency generation with a compressed, 20-fs pulse, revealing the appearance of an X-type wave shape.

Modern studies of nonlinear optics and wave propagation in general are paying increasing attention to regimes where ultrashort pulses coexist with extremely narrow transverse confinement. In this case a rich phenomenology can be envisaged, which can be neither predicted nor described by separating the dependence on space and time, as often assumed. Most of these new processes, in fact, appear to be ruled by a dominant angular dispersion (i.e., dependence of temporal frequency on angle), which is at the origin of the existence of propagation-invariant X-wave solutions of the linear wave equation in dispersive media [1] or solitonlike tilted-front pulses in the nonlinear regime [2]. This scenario makes the traditional concept of pulse and beam monitoring no longer adequate and demands high-resolution spatiotemporal (ST) three-dimensional-mapping (3DM) techniques to be adopted. A relevant example is the formation of X-shaped waves in the nonlinear regime, which has been invoked to interpret the apparent spatiotemporal collapse occurring in mismatched second-harmonic generation (SHG) [3,4], accompanied by temporal broadening (in air) and sub-Gaussian diffraction [5]. Nonlinear X waves are indeed stationary localized wave packets (WP's) which have shown to play a key role in the ST dynamics in focusing media with normal group-velocity dispersion (GVD) or dominant group-velocity mismatch (GVM) [3–6]. These WP's are supported by a strong interplay of space and time, which treated instead separately would lead to the erroneous conclusion that ST trapping cannot take place under the same conditions (plane-wave pulses would broaden in time). This interplay is also behind colored conical emission which can trigger their formation [7].

In this paper our aim is to describe in details the novel ST-3DM technique with fs resolution which allowed us to give unequivocal evidence that the ST compressed wave observed in the SHG experiment [3–5] is indeed an X wave with conical structure. Such a technique can be employed,

however, in a more general context where the spatial structure of a beam needs to be temporally resolved. The goal of a 3DM technique is that of acquiring a high-resolution snapshot of the intensity distribution of a *3D-localized*, highly structured WP. In the laboratory frame, 3DM should indeed give the WP intensity distribution $I(x,y,z,t)$ at a given time $t=t_0$, or, equivalently, in the coordinate system moving at WP group velocity v, with the retarded time defined as $\tau = t - z/v$, the technique should provide $I(x,y,z,\tau)$ at a given plane $z=z_0$. Therefore the goal of 3DM is conceptually different from the one related to monitoring the wavefront propagation in the quasi-cw regime [8], the propagation variable being treated as a fixed parameter in the present case. Recently, different experimental methods have demonstrated ps-3DM by means of down- [9], or up- [10] conversion gates, while in the fs range 2DM (e.g., limited to $y=y_0$) [11–13], as well as 3DM [14], has been reported employing nonlinear or linear techniques. Specifically the approach of Ref. [14], which exploits a cw source with ultrashort coherence time, was applied to measure nonparaxial linear X waves which, unlike our nonlinear X waves, are characterized by superluminal features. This method requires propagation invariance over several cm [14]. Conversely, the approach described in this paper, based on the nonlinear mixing of the WP to be characterized with a compressed, coherent, broad-area pulse (henceforth probe), allows us to obtain the fs-3DM of the WP at a fixed plane. This is relevant for WP's that are severely distorted with propagation.

Figure 1 displays the scheme of our experimental setup. The layout contains four different blocks: (i) generation of the X-type wave, (ii) generation of the probe, (iii) nonlinear gate, and (iv) detection. (i) The X wave is formed by launching 100-fs, 1060-nm, 45-μm [full width at half maximum (FWHM)], 0.3-μJ pulses in a 22-mm lithium triborate (LBO) crystal, tuned for SHG with positive phase mismatch $\Delta k = 2k(\omega) - k(2\omega)$, normal GVD, and large GVM [3]. The input pulses are generated by a frequency doubled parametric generator (TOPAS, Light Conversion Ltd), pumped by 100-fs Ti:sapphire laser pulses at a 1-kHz repetition rate. (ii) The high-contrast 20-fs, 650-nm, 4-mm, 10-μJ probe pulses

*Permanent address: Department of Physics and Nuclear Engineering, Universitat Politècnica Catalunya, 08222 Terrassa, Spain.
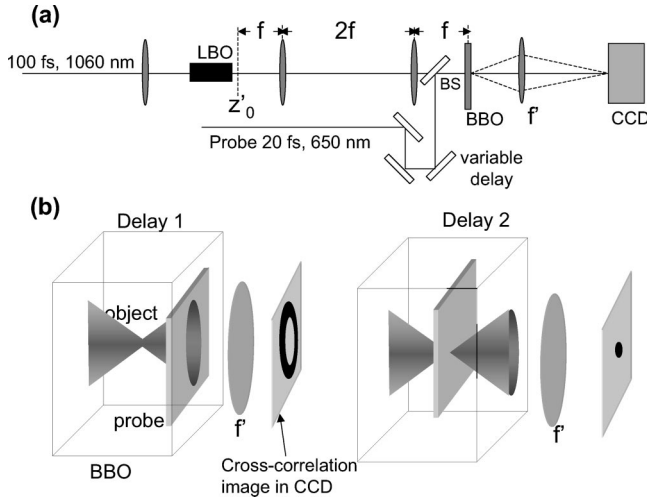
FIG. 1. (a) Experimental layout and (b) schematic representation of the cross-correlation nonlinear gating technique.

are provided by a noncollinear optical parametric amplifier (TOPAS White, Light Conversion Ltd), based on continuum seeding, chirped amplification, and final pulse compression, pumped by the second-harmonic pulses from the same Ti:sapphire laser. The pulse duration of the probe is 5 times shorter than the temporal dimensions of the WP to be measured. The autocorrelation trace of this pulse is plotted in Fig. 2 showing a clean Gaussian profile. (iii) The nonlinear gate is obtained by frequency mixing the output X wave with the 20-fs plane probe in a thin (20-μm-long) type-II β-barium borate (BBO) crystal. A 4-f telescope is used for imaging the field profile onto the BBO crystal plane in order to avoid the severe distorsion experienced by the X wave during free-space (air) propagation [5], with the lens thickness and aperture chosen in such a way to ensure minimum distortion. In the moving reference frame, for a retarded time τ_1, which corresponds to a given delay, the probe pulse crosses the BBO crystal while overlapping with a temporal slice of the (longer) X wave (GVM between the two WP's being negligible for such a thin crystal). Two examples for different delays are sketched in Fig. 1(b). In this configuration, the field obtained via sum-frequency generation (SFG) in the BBO results in a fluence distribution $F_{SFG}(x,y.;\tau_1)$ corresponding to the given delay τ_1. In order to obtain a SFG fluence proportional to the object intensity $I(x,y.,z_0,\tau_1)$, where z_0 corresponds to the fixed plane selected by the imaging telescope ($z_0=0$ at the LBO output-
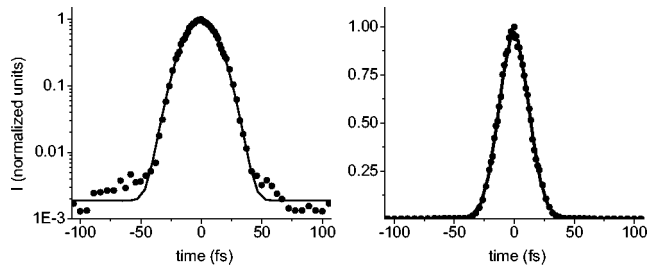
face plane), we need to employ a probe with constant intensity over the area of the WP to be characterized, as well as SFG to operate in the low-conversion limit [10]. All these constraints are well satisfied in our experiment. Then, by spanning the delay τ (we use 5-fs steps), the complete intensity map $I(x,y.,z_{0},\tau)$ can be retrieved, the ultimate temporal resolution being defined by the probe width, by its front steepness, and by its background. The quality of the used probe pulse, free from any substructure, shoulders, satellites, or slowly decaying tails (see the linear and logarithmic plots in Fig. 2), played a major role in leading to the largest possible temporal resolution, for the given FWHM probe-pulse duration. Indeed the shortest measured rise time (from $1/e$ to the peak), which corresponds to the steep leading edge of our WP, was 15 fs. This value has to be taken as an indicative estimation of the actual temporal resolution directly achievable with our setup. However, thanks to the high quality and high reproducibility of our probe pulse and to the fine step used, an even higher resolution can be obtained if data deconvolution will be performed by suitable algorithms. (iv) Finally the acquisition is performed by imaging the BBO-crystal plane on a charge-coupled-device (CCD) detector and by acquiring the fluence profile $F_{SFG}(x,y;\tau)$ for different τ. The proper magnification should be selected for the imaging system in order to avoid the pixel size of the camera limiting too much the final spatial resolution of the intensity profile (in our case a final spatial resolution close to 5 μm was achieved). The use of a high-dynamic (16-bit/pixel), low-noise (cooled at $-50\,°C$) CCD allowed us to obtain high sensitivity and high dynamic range detection, while keeping a very low conversion in the SF process. Typically, CCD on-chip integration over a few thousand shots was performed. The different intensity levels present in the WP could be recorded by simply changing the integrated number of shots for each temporal slice, keeping the probe intensity level always constant.

Figure 3 describes the results concerning the 3DM of the nonlinear X wave. Figure 3(a) shows a set of SFG fluence profiles $F_{SFG}(x,y;\tau)$ as recorded by the CCD, for different delays τ, while Fig. 3(b) shows the reconstructed spatiotemporal fluence profile in the vertical plane, $F_{SFG}(x=0,y;\tau)$. A representation of the WP profile in real physical (3D) space is given by selecting a particular intensity value and plotting the corresponding iso-intensity surface. An example for an intensity corresponding to 7% of the peak is reported in Fig. 3(c). In the measurement, the imaging telescope was settled for $z_0=+5$ mm, capturing the X-wave profile after it was propagated 5 mm in air, outside the LBO crystal. Measurements at $z_0=0$ revealed saturation in the SF process due to the too large peak intensity of the X wave. According to our simulations, the peak intensity drops by 3 times in 5 mm due to diffraction and shape-induced dispersion, without modifying substantially the overall shape of the WP. In the figure, we plot for comparison the results of a calculation performed under conditions identical to those in the experiment, accounting also for the free-space propagation and for the mixing with the 20-fs probe. The results are plotted in Fig. 3(b) (see right frame) and Fig. 3(c) (right frame), from which excellent agreement with the experiment is found.
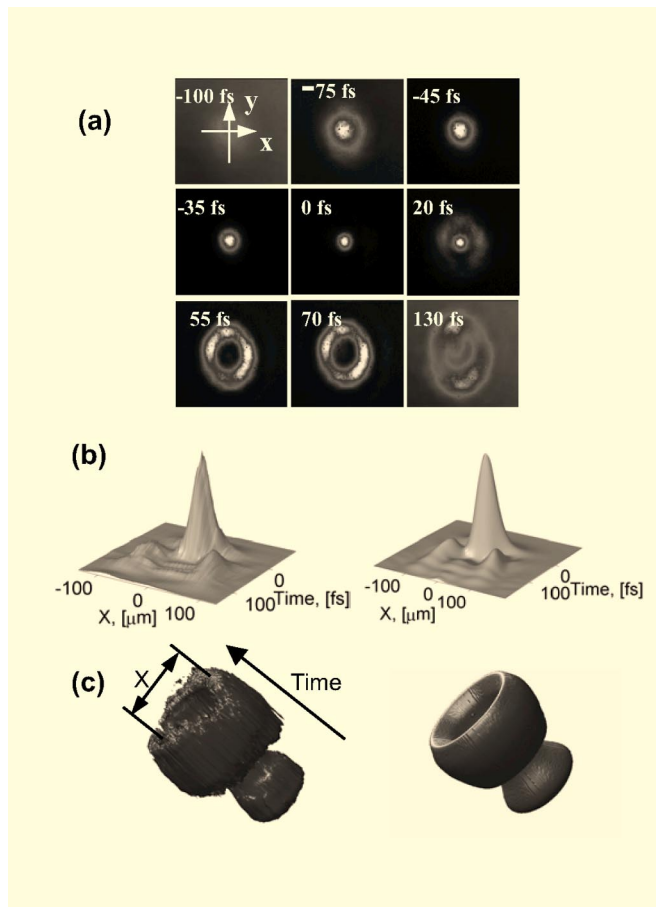

FIG. 2. Autocorrelation trace of the probe pulse in logarithmic and linear scale.

FIG. 3. (a) Transverse profiles of SFG fluence for different delays, (b) experimental (left) and simulated (right) intensity map of the X wave as captured after 5 mm of free-space propagation, and (c) experimental (left) and simulated (right) iso-intensity surface at the intensity level $0.07I_{\max}$.

They clearly show the X-type or conical-like shape of the WP, particularly well formed at the trailing edge of the pulse. On the leading edge, the WP exhibits a very steep front, from which we estimate for our setup a temporal resolution below 15 fs. Numerical calculations, whose detailed results will be presented elsewhere, show that more symmetrical WP's can be obtained for slightly different input focusing conditions, as well as when the $X^{(2)}$ interaction takes place without GVM [6].

Even if the setup is designed for 3DM purposes, time-integrated fluence profiles of the WP are also accessible: by simply closing the probe path and choosing suitable color filters, both the fundamental and second-harmonic profiles
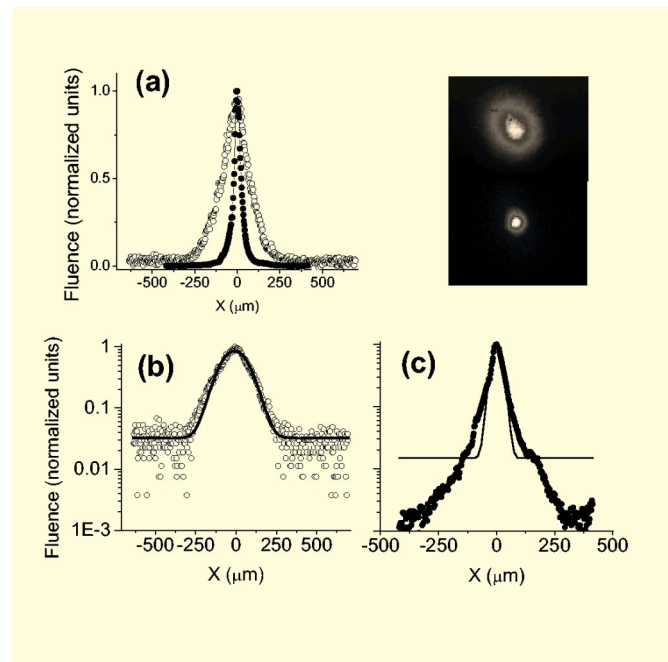

FIG. 4. (a) Time-integrated fluence transverse profiles of the formed X pulses at the output of LBO crystal for the fundamental wavelength in linear (open circles) and nonlinear (solid circles) regime. Gaussian fit (solid line) of the linear (b) and nonlinear (c) regimes showing the non-Gaussian distribution in the nonlinear case. Inset: CCD images for the two cases.

were measured. An example of the former is given in Fig. 4. The results make evident nonlinear beam compression, accompanied by a non-Gaussian redistribution of the WP fluence. Comparison between Figs. 4(a) and 4(c) shows how relevant is the high-dynamic range of the detector in disclosing the actual features of the WP.

In summary, by using an optical gate, based on a cross-correlation technique between the object and a much shorter probe broad-area pulse, combined with a high-dynamic CCD, we were able to obtain a 3D intensity map of the X wave spontaneously generated in a quadratic nonlinear interaction with resolution of 5 μm and 15 fs.

[1] H. Sonajalg, M. Ratsep, and P. Saari, Opt. Lett. **22**, 310 (1997).

[2] F. Wise and P. Di Trapani, Opt. Photonics News **13**, 28 (2002).

[3] P. Di Trapani, G. Valiulis, A. Piskarskas, O. Jedrkiewicz, J. Trull, C. Conti, and S. Trillo, Phys. Rev. Lett. **91**, 093904 (2003).

[4] G. Valiulis, J. Kilius, O. Jedrkiewicz, A. Bramati, S. Minardi, C. Conti, S. Trillo, A. Piskarskas, and P. Di Trapani, in *Proceedings of the Quantum Electronics and Laser Science Conference (QELS 2001)* (Optical Society of America, Washington, D.C., 2001).

[5] O. Jedrkiewicz, J. Trull, G. Valiulis, A. Piskarskas, C. Conti, S. Trillo, and P. Di Trapani, Phys. Rev. E **68**, 026610 (2003).

[6] C. Conti, S. Trillo, G. Valiulis, A. Piskarskas, O. Jedrkiewicz, J. Trull, and P. Di Trapani, Phys. Rev. Lett. **90**, 170406 (2003).

[7] S. Trillo, C. Conti, P. Di Trapani, O. Jedrkiewicz, J. Trull, G. Valiulis, and G. Bellanca, Opt. Lett. **27**, 1451 (2002).

[8] S. G. Pettersson, H. Bergstrom, and N. Abramson, Appl. Opt. **28**, 766 (1989).

[9] F. Devaux and E. Lantz, Opt. Commun. **118**, 25 (1995).

[10] M. Potenza, S. Minardi, J. Trull, G. Blasi, D. Salerno, P. Di Trapani, A. Varanavicius, and A. Piskarskas, Opt. Commun. **229**, 381 (2004).

[11] M. Fujimoto, S. Aoshima, M. Hosoda, and Y. Tsuchiya, Opt. Lett. **24**, 850 (1999).

[12] L. Gallman, G. Steinmeyer, D. H. Sutter, T. Rupp, C. Iaconis, I. A. Walmsley, and U. Keller, Opt. Lett. **26**, 96 (2001).

[13] T. Tanabe, H. Tanabe, Y. Teramura, and F. Kannari, J. Opt. Soc. Am. B **19**, 2795 (2002).

[14] P. Saari and K. Reivelt, Phys. Rev. Lett. **79**, 4135 (1997).